Essential role of insulin-like growth factor 2 in resistance to histone deacetylase inhibitors

Su-Chan Lee[1,4], **Hye-Young Min**[1,4], **Hyun Jin Jung**[2], **Kwan Hee Park**[1], **Seung Yeob Hyun**[1], **Jaebeom Cho**[1], **Jong Kyu Woo**[1], **So Jung Kwon**[3], **Hyo-Jong Lee**[3], and **Ho-Young Lee**[1,2,*]

[1]College of Pharmacy and Research Institute of Pharmaceutical Sciences, Seoul National University, Seoul 08826, Republic of Korea

[2]Interdisciplinary Program in Genetic Engineering, Seoul National University, Seoul 08826, Republic of Korea

[3]College of Pharmacy, Inje University, Gimhae, Gyungnam 50834, Republic of Korea

Abstract

Histone deacetylase inhibitors (HDIs) are promising anticancer therapies and have been clinically used for the treatment of hematological malignancy. However, their efficacy in solid tumors is marginal and drug resistance hampers their further clinical utility. To develop novel strategies for the HDI-based anticancer therapeutics in non-small cell lung cancer (NSCLC), in the present study, we investigated the mechanisms underlying resistance to HDI treatment in NSCLC cells. We show the STAT3-mediated IGF2/IGF-1R signaling cascade as a key modulator for both acquired and primary HDI resistance. Treatment with HDI up-regulated *IGF2* transcription in NSCLC cells carrying intrinsic or acquired drug resistance via direct binding of STAT3 in *IGF2* P3 and P4 promoters. Acetylated STAT3 emerged upon HDAC inhibition was protected from the proteasome-mediated degradation of STAT3 and functioned as a direct transcription factor for *IGF2* expression. Genomic or pharmacological strategies targeting STAT3 diminished the HDI-induced IGF2 mRNA expression and overcame the resistance to HDI treatment in HDI-resistant NSCLC- or patient-derived tumor xenograft models. These findings provide new insights into the role of acetylated STAT3-mediated activation of *IGF2* transcription in HDI resistance, suggesting IGF2 or STAT3 as novel targets to overcome HDI resistance in NSCLC.

Keywords

insulin-like growth factor 2; histone deacetylase inhibitor; drug resistance; signal transducer/transcription factor 3; non-small cell lung cancer

---

*Correspondence to: Ho-Young Lee, Ph.D., College of Pharmacy and Research Institute of Pharmaceutical Sciences, Seoul National University, 1 Gwanak-ro, Gwanak-gu, Seoul 08826, Republic of Korea, Phone: +82-2-880-9277; Fax: +82-2-6280-5327; hylee135@snu.ac.kr.
4These two authors contributed equally to this work and should be considered as first author.

Introduction

Histone deacetylase (HDAC) inhibitors (HDIs) have been anticipated to exert substantial anticancer activity by selectively inducing transcriptional restoration of epigenetically silenced tumor suppressor genes through transcription-dependent and transcription-independent mechanisms involving hyperacetylation of histones and non-histone proteins[27]. Indeed, a small subset of patients with solid or hematologic malignancies enrolled in clinical trials have shown encouraging responses to vorinostat (suberoylanilide hydroxamic acid), the first US Food and Drug Administration-approved class I and II HDI[5, 9, 29, 30, 42]. However, drug resistance is a major concern for the use of HDIs in anticancer therapeutics[7, 18]. Among various potential mechanisms underlying HDI resistance, DNA hypermethylation represents a mechanism of resistance uniquely relevant to HDIs. Combining two epigenetic drugs targeting DNA methyltransferase (DNMT) and HDAC with chemotherapy has shown clinical benefit for the treatment of hematologic malignancies[14]. However, the mechanism of HDI resistance in solid tumors has been poorly investigated.

Deregulated expression of insulin-like growth factor 2 (IGF2) and activation of the type 1 IGF receptor (IGF-1R) signaling network have been implicated in cell proliferation, survival, and maintenance of self-renewal of cancer stem cells, contributing to resistance to several types of anticancer regimens[2, 3, 6, 11, 36, 44]. Overexpression of IGF2 is frequently due to loss of imprinting (LOI)[15, 32, 40], in which methylation of the imprinting control region (ICR)[1, 10, 31] abrogates the binding of zinc finger protein CTCF, which acts as an insulator that sequesters enhancers downstream of *H19* to suppress *IGF2* transcription[34]. IGF2 expression may be also deregulated by transcription factors, such as E2f3 and ZFP57[22, 41]. However, the transcriptional modulation of IGF2 besides genomic imprinting still needs to be investigated.

In a previous study, we demonstrate that activation of IGF-1R signaling is associated with primary vorinostat resistance in NSCLC[13]. According to the previous results, in the present study, we report the novel finding that deregulated IGF2 overexpression through a novel mechanism that involves STAT3 mediates intrinsic and acquired resistance to HDI. Mechanistically, acetylation (K685)-mediated stabilization of STAT3 protein upon HDAC inhibition cause a transcriptional up-regulation of *IGF2*. Targeting STAT3 effectively overcame vorinostat resistance in NSCLC cells and in NSCLC- or patient-derived tumor xenografts. Our results suggest that targeting the STAT3-IGF2 axis is an effective strategy to overcome HDI resistance in NSCLC.

Results

The IGF-1R pathway is directly involved in primary and acquired vorinostat resistance in NSCLC cells

In our previous report, we differentiated a panel of 12 human NSCLC cells based on the cell response to vorinostat treatment. In the current study, we chose 3 vorinostat-sensitive cells (H1944, H322, H358 cells) and generated their sublines (VoR) carrying acquired drug resistance to vorinostat by treating the cell lines with increasing doses of vorinostat for > 6 months. The VoR sublines displayed significantly increased viability (Figure 1a), anchorage-

independent colony-forming ability (Figure 1b), and markedly decreased caspase-3 cleavage (Figure 1c) upon vorinostat treatment, suggesting successful acquisition of drug resistance. Notably, a VoR subline H1944R showed a cross resistance to another HDI, romidepsin (depsipeptide) (Figure 1d). We investigated the mechanisms involved in acquired resistance to vorinostat. Consistent with our previous results in NSCLC cells with primary resistance to vorinostat[13], treatment with vorinostat induced a dose-dependent up-regulation of IGF-1R phosphorylation in the VoR sublines but not in the parental vorinostat-sensitive cells (Figure 1e). Moreover, the inhibitory effects of vorinostat on the colony-forming ability of the VoR cells were significantly enhanced by treatment with an anti-IGF-1R monoclonal antibody (mAb) (Figure 1f). Together with our previous observation, these results suggest that the IGF-1R signaling pathway plays a key role in both primary and acquired vorinostat resistance.

Vorinostat increases *IGF2* transcription in cells with primary and acquired vorinostat resistance

We investigated the mechanisms underlying vorinostat-induced IGF-1R activation. Because the vorinostat-induced IGF-1R activation was not followed by an increase in IGF-1R expression (Figure 1e), we analyzed the effects of vorinostat treatment on IGF1 and IGF2 expression in the vorinostat-sensitive parent cells and their sublines. Vorinostat treatment was found to induce significant increases in the transcription of *IGF2*, but not *IGF1*, in the VoR sublines compared with their parental cells (Figure 2a). Vorinostat-induced *IGF2* transcription was also observed in various cell lines with primary vorinostat resistance (Figure 2b). An elevated IGF2 secretion upon vorinostat treatment was confirmed with supernatants from representative primary (H226B) or acquired (H1944R and H322R) vorinostat resistant cells (Figure 2c). Notably, silencing IGF2 expression by siRNA transfection (Figure 2d) prevented vorinostat-induced IGF-1R activation (Figure 2e) and restored vorinostat sensitivity in vorinostat-resistant cells, which was comparable with the effect of vorinostat on H1944 cells at the same concentration (Figure 2f), suggesting the involvement of IGF2 in both primary and acquired resistance against vorinostat.

Recruitment of STAT3 to the P3 and P4 promoters plays a crucial role in *IGF2* transcription upon HDAC inhibition

Human *IGF2* transcription is modulated by four alternate promoters (P1—P4)[28, 43], of which P3 and P4 are predominant in most tissues[43]. RT-PCR using 5' primers specific for each of the four *IGF2* promoters, which gives distinct transcript variants of IGF2, and a common 3' primer on exon 7 (Figure 3a) revealed that P3 and P4 promoters directed the vorinostat-induced *IGF2* transcription in NSCLC cells with acquired or primary vorinostat resistance (Figure 3b). Luciferase reporter assays further confirmed vorinostat-induced activation of the P3 and P4 promoters (Figure 3c). The P3 and P4 promoters were also employed for the *IGF2* transcription by other clinically available HDIs, including entinostat, panobinostat, and romidepsin, in both primary (H226B) and acquired (H1944R) vorinostat-resistant NSCLC cells (Figure 3d). These findings suggest that P3 and P4 promoter-mediated *IGF2* transcription is a general response to HDAC inhibition and is closely related to the resistance to HDIs.

STAT3 induces HDI-induced IGF2 expression, eventually leading to resistance to HDI treatment in NSCLC

We assessed the factors responsible for *IGF2* transcription upon HDAC inhibition. In light of our recent finding on the association of STAT3 with IGF2 expression[19], the implication of STAT3 in *IGF2* transcription in myoblasts[45], and the suggested association of STAT3 with HDI resistance in cutaneous T-cell lymphoma[8], we postulated the implication of STAT3 in *IGF2* transcription and vorinostat resistance. Indeed, genomic (siRNA) (Figure 4a) or pharmacological (Stattic[35]) (Figure 4b) inactivation of STAT3 significantly attenuated the vorinostat-induced *IGF2* transcription, especially those directed by the P3 and P4 promoters (Figure 4c). The P3 and P4 promoter activities were also significantly suppressed by the Stattic treatment (Figure 4d). These findings indicated the involvement of STAT3 in *IGF2* transcription through P3 and P4 promoters. The inhibitory effects of vorinostat on the anchorage-dependent colony formation (Figure 4e) and tumor growth (Figure 4f) were significantly enhanced when STAT3 expression was silenced by the STAT3-specific shRNA. Moreover, significant combinatory antitumor effects of vorinostat and Stattic were observed in NSCLC patient-derived xenograft tumors (PDXs) (Figure 4g). These data suggest that increased STAT3 activity plays a key role in *IGF2* transcription and vorinostat resistance.

STAT3 directly binds to P3 and P4 promoter of *IGF2* gene, leading to HDI-induced IGF2 transcription

We investigated whether STAT3 directly binds to *IGF2* promoter for the transcriptional regulation of the gene. Indeed, the JASPAR database predicted one (P3-S1) and six (P4-S1 to P4-S6) potential STAT3-binding sites in the *IGF2* P3 and P4 promoters, respectively (Figure 5a). The colorimetric DNA-binding ELISA (DELISA) using DNA sequences that encompass the seven potential STAT3-binding regions within the promoters revealed that vorinostat treatment significantly increased STAT3 binding to the P3-S1, P4-S3/4, and P4-S5/6 (Figure 5b). The specificity of this binding was confirmed by competition assay using excess wild-type (WT) but not mutant (M) oligomers (Figure 5c). The ChIP assay also demonstrated the STAT3 occupancy to the potential sites (Figure 5d). Moreover, mutation of potential STAT3 binding sites resulted in significant ablation of vorinostat-induced activation of *IGF2* P3 and P4 promoters (Figure 5e). These results indicate the direct binding of STAT3 in *IGF2* P3 and P4 promoters, thereby leading to increase *IGF2* transcription and subsequent drug resistance upon vorinostat treatment.

STAT3 protein acetylation upon HDAC inhibition is crucial for its stabilization and thus for IGF2 expression

We determined the mechanisms by which STAT3 mediates vorinostat-induced *IGF2* transcription. Notably, vorinostat treatment increased expression and acetylation (K685), but not phosphorylation (Y705), of STAT3 protein in both vorinostat-sensitive H1944 cells and all of vorinostat-resistant cells (Figure 6a). We then assessed the impact of acetylation on STAT3 function by employing H1299 cells, in which endogenous STAT3 was stably depleted by shRNA transfection and then wild type (WT) or acetylation-null mutant STAT3 (K685R) were introduced. Vorinostat treatment induced time-dependent increases in both total and acetylated STAT3 (Ac-STAT3) primarily in the nuclear compartment (Figure 6b),

which were abrogated by the STAT3 mutation (K685R) (Figure 6c). In line with the findings, vorinostat-mediated increases in transcription (Figure 6d) and P3 and P4 promoter activities (Figure 6e) and secretion (Figure 6f) of IGF2 were attenuated by the STAT3 mutation. Immunofluorescence staining further confirmed markedly decreased IGF2 expression and nuclear Ac-STAT3 contents by the STAT3 mutation (Figure 6g). Moreover, abrogation of STAT acetylation substantially enhanced vorinostat's effects on apoptosis (Figure 6h) and colony formation (Figure 6i). These results suggest that IGF2 expression upregulated by increased STAT3 acetylation is crucial for vorinostat resistance.

Intriguingly, the STAT3 mutation decreased both Ac-STAT3 and STAT3 levels (Figures 6c and 6h). Hence, we addressed the effects of the mutation (K685R) on half-life of STAT3. Surprisingly, the half-life of STAT3 protein was dramatically decreased by the mutation (Figure 6j). Moreover, treatment with a proteasome inhibitor MG132 increased the levels of ubiquitinated form of the STAT3 mutant. The mutant STAT3 protein levels were also increased by the MG132 treatment (Figure 6k). These data suggest that increased STAT3 activity through the acetylation-mediated protein stabilization from proteasome-mediated degradation plays a key role in *IGF2* transcription and vorinostat resistance.

Discussion

Despite considerable enthusiasm about the use of HDIs as an anticancer therapy, several clinical trials have shown poor responses to these drugs. However, molecular determinants of resistance to HDIs, especially those responsible for acquired resistance due to chronic exposure to HDIs, are poorly understood. Understanding the mechanisms that determine resistance to HDIs would grant the basis for therapeutic combinations with improved clinical efficacy. In the current study, we show that transcriptional up-regulation of *IGF2* via acetylated STAT3 play a key role in both de novo and acquired resistance to HDIs. We propose that HDAC inhibition increases functional STAT3 levels in the nuclear compartment through acetylation-mediated protein stabilization, leading to P3/P4 promoter-mediated *IGF2* transcription. We also show that blockade of STAT3 effectively suppresses the HDI-induced *IGF2* transcription and potentiates the therapeutic efficacy of HDIs in human NSCLC cells and PDXs. To our knowledge, this is the first study to demonstrate the deregulated function of STAT3 through acetylation as a determinant of IGF2 transcription and HDI resistance.

HDIs are known to alter function of various proteins, thereby regulating expression of tumor suppressor genes and interfering with cancer cell proliferation and survival. However, cancer cells are highly adjustable - a feature that enables them to cope with such inhibitory constraints and thus contributes to the development of drug resistance. Here we demonstrate that, in both acquired and de novo HDI-resistant tumors, transcriptional increase in IGF2 plays a universal role in activation of the IGF-1R pathway and thus mediating resistance to HDIs. We show that: 1) various HDIs led to the transcriptional increase in *IGF2* expression in both primary and acquired HDI-resistant NSCLC cells through P3- and P4-directed promoter activities; and 2) knock-down IGF2 expression sensitized both primary and acquired vorinostat-resistant cells to the drug treatment, indicate an IGF2 dependency of NSCLC for HDI resistance. These findings are in line with the previous report showing

ineffectiveness of HDIs to induce apoptosis through activation of the Akt pathway[13, 24]. Under that scenario, one could design approaches targeting IGF-1R as a therapeutic option to overcome HDI resistance. However, IGF-1R targeting by monoclonal antibody (mAb) or tyrosine kinase inhibitor (TKI) has been challenging due to weak efficacy and drug resistance through various mechanisms[26, 37, 38]. Thus, we propose that, instead of targeting IGF-1R, understanding the IGF2 biology and identifying the key factors involved in HDI-induced IGF2 transcription would be practical to develop therapeutic strategies overcoming the HDI resistance.

Previously, STAT3 has been suggested as a factor for HDI resistance in hematologic cancer[8]. However, functional significance, downstream effectors, and therapeutic merits of targeting STAT3 in HDI resistance have been elusive. Our IGF2 promoter studies both primary and acquired HDI-resistant cells reveal a direct binding of STAT3 to the P3/P4 *IGF2* promoters and the STAT3 dependency of the NSCLC cells for the HDI-induced *IGF2* transcription. Moreover, genomic and pharmacologic approaches targeting STAT3 effectively suppressed the HDI-induced *IGF2* transcription and restored drug sensitivity in both primary and acquired HDI-resistant cells. Most importantly, inactivation of STAT3 universally suppresses the vorinostat-induced *IGF2* gene expression and restores vorinostat sensitivity in both primary and acquired HDI-resistant NSCLC cells and PDXs. These findings indeicated the universal role of STAT3 in NSCLC cells' resistance to HDIs.

In our study, HDAC inhibition was found to cause a rapid STAT3 acetylation (K685), protecting STAT3 from the proteasome-mediated degradation, and increase in its nuclear localization and the activity as a transcriptional factor. Previous studies have demonstrated STAT3 acetylation by histone acetyltransferase p300[17, 48]. The role of STAT3 acetylation at at a single lysine residue (K685) in its dimerization has been reported[17, 48, 49]. Therefore, it is likely that HDAC inhibition results in stabilization of STAT3 through acetylation, leading to increases in its dimerization and activity as a transcription factor. These results support the role of STAT3 as a direct transcription factor for *IGF2* expression, placing it as a key node for HDI resistance. In addition to the IGF2-IGF-1R pathway, STAT3 modulates numerous genes thereby playing diverse roles in cancer cell proliferation, survival, and metastasis[4]. Together, these findings endorse the broad clinical utility of the combinatorial therapy with HDI and STAT3 in HDI-based clinical trials. However, increases in both total and acetylated STAT3 were also found in vorinostat-sensitive cells (Figure 6a), implying the existence of an additional factor associated with vorinostat resistance. Further studies are underway to investigate additional determinants of vorinostat resistance.

In conclusion, we reveal the role of the STAT3-IGF2 axis in both de novo and acquired resistance to HDIs. The combinatorial regimens of HDIs with STAT3-targeted drugs are effective in both primary and acquired HDI resistance. As some STAT3 inhibitors and IGF2 neutralizing antibodies have been recently investigated in clinical trials[46, 47], our findings will have a direct impact on the relevant clinical trials with HDIs. In addition, considering the immunomodulatory properties of HDIs[20], understanding the properties of the IGF2-IGF-1R axis in compromising the antitumor effects of HDIs would be also important for combinatorial anticancer therapeutics using HDIs and other anticancer agents including

immuomotherapeutic agents. Further clinical investigations evaluating the effectiveness of the novel combinatorial strategies are warranted.

Materials and Methods

Cells and Reagents

Human NSCLC lines H226B, H226Br, H322, H358, H1299, and H1944 were purchased from the American Type Culture Collection (ATCC; Manassas, VA, USA) or kindly provided by Dr. John V. Heymach (MD Anderson Cancer Center, Houston, TX, USA). Cells were cultured in RPMI 1640, supplemented with 10% fetal bovine serum (FBS, Welgene, Daegu, Republic of Korea) and antibiotics at 37°C in a humidified environment with 5% CO_2. Cells were authenticated using AmplFLSTR identifier PCR Amplification Kit (Applied Biosystems, Foster, CA; cat. No. 4322288) in 2013 and 2014. We used cells passed for fewer than 6 months after resuscitation of validated cells. Vorinostat was purchased from Cayman (Ann Arbor, MI, USA). Chemicals unless otherwise indicated were purchased from Sigma-Aldrich (St. Louis, MO, USA).

Establishment of vorinostat-resistant cell Lines

For generating H1944R cells, H1944 cells were exposed to 0.2 μM vorinostat for 48 h in RPMI 1640 medium containing 10% FBS, washed, and then cultured in drug-free medium until the surviving population of cells re-established 80% confluence. The process was repeated for 2 months with sequentially increased dosages of vorinostat (0.5-5 μM). The established resistant cell line (H1944R) was maintained by culture in a medium containing 5 μM vorinostat. In addition, vorinostat-resistant H358 and H322 cells (designated 'R') were established as follows. H358 and H322 cells were treated with gradually increasing concentrations of vorinostat (0.1 to 2 μM) for more than 6 months. For all the in vitro studies, the resistant cells were cultured in drug-free medium for at least 1 week to eliminate the effects of vorinostat.

Cell viability assay

Cells were seeded into 96 well plates at a density of $1\text{-}2 \times 10^3$ cells/well. Cells were treated with vorinostat for 3 days. Cells were incubated with the MTT solution (final 200-500 μg/ml) for 3 h at 37°C. The formazan crystals were dissolved in DMSO and the absorbance was measured at 570 nm.

Anchorage-independent colony formation assay

Cells (5×10^3 cells/well for H322 and H358 cells; 2×10^3 cells/well for other cells) were mixed with the low-melting agar solution (final 0.4%; top agar). and 500 μl of cell suspension was poured onto 500 μl of 1% base agar solidified in 24 well plates prior to the experiment. After solidification of the top agar, more than 500 μl of drug-containing medium was added to the agar and incubated for 2 weeks. Colonies were stained with 500 μg/ml MTT solution, photographed, and counted using Image J software (National Institutes of Health, Bethesda, Maryland, USA)[33].

Anchorage-dependent colony formation assay

Cells (200 cells/well) were seeded into 6 well plates and then incubated for 10–15 days in complete medium containing the indicated concentration of test compounds. The medium was changed twice a week during this treatment period. After incubation, colonies were fixed with methanol and then stained with 0.005% crystal violet. Colonies were photographed and counted using Image J software.

Western blot analysis

Total cell lysates were prepared with modified RIPA lysis buffer (50 mM Tris-HCl [pH 7.4], 150 mM NaCl, 1 mM EDTA, 0.25% sodium deoxycholate, 1% Triton X-100, 100 mM NaF, 1mM Na3VO4, and protease inhibitor cocktail [Roche Applied Science, Indianapolis, IN, USA]). To prepare cytosolic and nuclear fractions, we used buffer A (10 mM HEPES [pH 7.9], 10 mM KCl, 1.5 mM MgCl2, 1 mM DTT, 0.1% NP-40, and protease inhibitor cocktail) and buffer C (20 mM HEPES [pH 7.9], 420 mM NaCl, 20% glycerol, 1 mM EDTA, and protease inhibitor cocktail), respectively.

Equal amounts of lysates were subjected to 8–10% SDS-PAGE. Separated proteins were transferred onto a PVDF membrane (Bio-Rad Laboratories, Hercules, CA, USA). Membranes were blocked with blocking buffer (5% BSA in PBS containing 0.1% Tween-20 [PBST]) for 1 h at room temperature (RT) and followed by incubation with primary antibodies diluted in blocking buffer (1:1,000) overnight at 4°C. Membranes were washed with PBST and incubated with the corresponding secondary antibodies diluted in 3% non-fat dry milk in PBST (1:5,000) for 1–2 h at RT. Membranes were washed with PBST and were visualized using an enhanced chemiluminescence (ECL) detection kit (Thermo Fisher Scientific, Grand Island, NY, USA).

The following antibodies were used for Western blot analysis. Antibodies against pIGF-1R [Y1131 (catalog # 3021) or Y1135/6 (catalog # 3024)], IGF-1R (catalog # 3027), pSTAT3 (Y705; catalog # 9131), acetyl-STAT3 (catalog # 2523), STAT3 (catalog # 4904), PARP (catalog # 9542), α/β-tubulin (catalog # 2148), and cleaved caspase-3 (catalog # 9661) were purchased from Cell Signaling Technology (Danvers, MA, USA). Primary antibodies against IGF-1R (catalog # sc-713), actin (catalog # sc-1615), ubiquitin (catalog # sc-8017), GFP (catalog # sc-5385), and horseradish peroxidase (HRP)-conjugated secondary antibodies were purchased from Santa Cruz Biotechnology (Santa Cruz, CA, USA).

Cloning of *IGF2* P4 promoter luciferase reporter and STAT3 expression vectors

The *IGF2* P4 promoter luciferase reporter vector was constructed by subcloning a XhoI-Hind III fragment of the PCR product of genomic DNA of H1944 cells (PCR primers (forward, reverse): 5'-ATCTCGAGCACCCTGGTATGTTGACGC-3', 5'-ATAAGCTTTACAGCTCAGCAGAAGGCTC-3'; positions -546 to +102[39]) into pGL3-basic. The expressing vectors containing WT or mutant STAT3 were constructed by subcloning a EcoRI-Hind III fragment of rAAV-3xFlag WT or mutant murine STAT3 knock-in targeting vectors (kindly provided by Dr. Hua Yu at City of Hope Comprehensive Cancer Center, CA, USA)[17, 50] into pEGFP-N3.

Transfections

For knockdown of IGF-1R, IGF2, or STAT3 expression, cells were transiently transfected with either scrambled small interfering RNAs (siRNAs) (Shanghai GenePharma, Shanghai, China) or siRNAs targeting IGF2 or STAT3 (Dharmacon [Lafayette, CO, USA] or Shanghai GenePharma) using Lipofectamine RNAiMAX (Invitrogen, Carlsbad, CA, USA) according to the manufacturer's instructions. To generate stable knockdown cell lines with reduced STAT3 expression, H1299 cells were transduced with lentiviral particles with shRNA clones against STAT3 (Sigma-Aldrich) and then followed by antibiotic selection with puromycin. To generate H1299 cells transiently overexpressing wild type (WT) or acetylation-null mutant (mutant) STAT3, H1299 cells stably expressing reduced STAT3 were further transfected with empty vector (EV; pEGFP-N3), pEGFP-STAT3, or pEGFP-STAT3 K685R using Lipofectamine 2000 (Invitrogen) according to the manufacturer's instructions.

Reverse-transcription polymerase chain reaction (RT–PCR)

Total RNA was isolated using a phenol-chloroform extraction, reverse-transcribed, and analyzed by RT–PCR or a SYBR Green-based real-time PCR (LightCycler 480 real-time PCR system, Roche). The thermocycler conditions for RT–PCR were as follows: initial denaturation at 94°C for 5 min; 28–35 cycles of 94°C for 30 s, 55-60°C for 30 s, and 72°C for 30 s; final elongation at 72°C for 5-7 min. The thermocycler conditions for real-time PCR were as follows: pre-incubation at 95°C for 5 min, 50 cycles of 95°C for 10 s, 60°C for 10 s, and 72°C for 10 s, and melting curve analysis for determining reaction specificity. In addition, the promoter (P1–P4)-specific transcripts of the *IGF2* gene were analyzed as described in the previous report[16]. PCR products were separated by 2% agarose gel electrophoresis and visualized using a Gel Doc EZ System (Bio-Rad Laboratories, Hercules, CA, USA). Relative quantification of mRNA expression was performed by the comparative C_T (cycle threshold) method as described previously[21]. The primer sequences used for the PCR and the real-time PCR are described in Supplementary Tables S1-S3.

IGF2 ELISA

IGF2 ELISA was performed using a commercially available IGF2 ELISA kit (catalog # DSL-10-2600, Beckman Coulter, Indianapolis, IN, USA and catalog # KA3050, Abnova, Taipei City, Taiwan) according to the manufacturer's instructions.

Luciferase reporter assay

Reporter gene assay was performed using a luciferase assay system (Promega Corp. Madison, WI, USA) according to the manufacturer's protocol. Briefly, cells were co-transfected with pGL3-basic or luciferase vectors containing *IGF2* P3 and P4 promoter sequences (P3-Luc[39] or P4-Luc, respectively) and pSV-β-Gal. After treatment with vorinostat, cells were harvested with passive lysis buffer, and luciferase activity was monitored using a microplate luminometer (Berthold Technologies GmbH & Co. KG, Germany). β-galactosidase activity was measured using β-galactosidase enzyme assay system (Promega) and served as a control to normalize transfection efficiency.

Determination of protein stability and ubiquitin-mediated proteosomal degradation

To determine the impact of STAT3 acetylation on STAT3 protein stability, H1299 cells expressing WT or mutant STAT3 were treated with cycloheximide (CHX; 50 μg/ml) for 3, 6, and 9 h, and the level of total and acetylated STAT3 was determined by Western blot analysis. In addition, to examine the involvement of ubiquitin-mediated proteasomal degradation of STAT3 in the STAT3 destabilization, cells were exposed to MG132 (10 μM) for 6 h. Total STAT3 expression was determined by Western blot analysis. In addition, lysates were immunoprecipitated with anti-GFP antibodies, followed by Western blot analysis to detect the level of ubiquitination using anti-ubiquitin antibodies.

Immunofluorescence

Immunofluorescence staining was performed as described previously[12] using the antibodies against IGF2 and Ac-STAT3. Briefly, cells were seeded onto coverslip and treated with vorinostat for 2 days. Cells were fixed with 4% paraformaldehyde. Coverslips were incubated with the blocking buffer (5% BSA and 0.05% Tween-20 in TBS), and then incubated with anti-Ac-STAT3 or anti-IGF2 (EMD Millipore, Billerica, MA, USA) primary antibodies diluted in blocking buffer. After washing, coverslips were incubated with the corresponding FITC-conjugated secondary antibodies, washed, and then mounted with a mounting solution containing DAPI. The fluorescence was observed under the fluorescent microscope.

DNA ELISA

DNA ELISA was performed as described previously[25] with some modifications. ELISA plates pre-coated with annealed oligonucleotides corresponding to predicted STAT3-binding regions at the *IGF2* P3 and P4 promoters, identified using the JASPAR database[23], using React-Bind DNA coating solution (Thermo Fisher Scientific, Inc, Grand Island, NY, USA) for 1 h at RT. After blocking with the blocking buffer (4% BSA in PBS), nuclear extracts (5 μg/well), diluted in the dilution buffer (12 mM HEPES [pH 7.9], 60 mM KCl, 0.4 mM EDTA, 0.5 mM DTT, 12% glycerol, 35 μg/ml poly (dI-dC)), were added and incubated for 3 h at 4°C. After washing with TBST, primary antibodies (200 ng/ml anti-STAT3 antibodies in 4% BSA in PBS) were added to the plates and incubated for 1 h at RT. After washing with TBST, secondary antibodies (anti-rabbit-HRP [Bethyl Laboratories, Inc., Montgomery, TX, USA]; diluted in 1:20,000) were added to the plates and incubated for 30 min at RT. After washing with TBST, 50 μl of 3,3',5,5-tetramethylbenzidine (TMB) solution (Sigma-Aldrich) was added to each well and incubated for 20 min at RT. After adding stop solution (50 μl of 0.1 N HCl), absorbance was measured at 450 nm.

Chromatin immunoprecipitation (ChIP) assay

ChIP was performed using the SimpleChIP enzymatic chromatin IP kit (Cell Signaling Technology) according to the manufacturer's provided protocol. In brief, the chromatin cross-linked to proteins was digested with micrococcal nuclease. The digested chromatin was immunoprecipitated with control IgG or anti-STAT3 (Santa Cruz or Cell Signaling) antibodies. The DNA-protein cross-links of immunoprecipitants were reversed and then DNA was purified. The association between STAT3 and the potential STAT3-binding

regions at the *IGF2* P3 and P4 promoters, identified using the JASPAR database[23], was analyzed by PCR. The PCR primers used for ChIP are described in Supplementary Table S4. PCR products were subjected to 2% agarose gel electrophoresis and visualized using a Gel Doc EZ System (Bio-Rad).

Animal Studies

All animal procedures were performed using a protocol approved by the Seoul National University Institutional Animal Care and Use Committee. H1299 (stably transfected with shRNAs targeting STAT3) cells (5×10^6 cells/spot) were subcutaneously injected into the flanks of a 5–6-week-old female NOD/SCID mice. For PDX, small pieces of tumors derived from NSCLC patients were subcutaneously inoculated into the flanks of 5–6-week-old female NOD/SCID mice. After the tumor volume reached 50–150 mm^3, mice were randomly grouped to give equal mean tumor size and body weight in each group and intraperitoneally treated with vehicle (distilled water containing 10% DMSO and 45% polyethylene glycol 400) or drugs, alone or in combination, six times per week for 18 days in an unblinded fashion. Tumor growth was determined by measuring the short and long diameters of the tumor with a caliper, and body weight was measured twice per week to monitor toxicity. The tumor volume was calculated using the following formula: tumor volume (mm^3) = (short diameter)^2 × (long diameter) × 0.5.

Statistical Analysis

The data are presented as the mean ± SD. All in vitro experiments were independently performed at least twice, and a representative result is presented. We assessed the outcome of data in a blinded fashion. We carried out Student's *t*-test (unpaired, two-sided) using Microsoft Excel 2010 (Microsoft Corp., Redmond, WA, USA) to analyze the statistical significance of difference of in vitro data. We assumed the equal variance of each data in the statistical analysis using Student's *t*-test. One-way analysis of variance (ANOVA) followed by Newman-Keuls *post hoc* test using GraphPad Prism 5 (GraphPad Software Inc., La Jolla, CA, USA) was performed to analyze the statistical significance of difference of in vivo data. We could not analyze normal distribution of data using D'Agostino and Pearson normality test due to sample size. We did not perform power analysis to estimate sample size. The total sample size ('*n*') and statistical method are indicated in figure legends. *P* values less than 0.05 were considered statistically significant.

Supplementary Material

Refer to Web version on PubMed Central for supplementary material.

Acknowledgments

References

1. Bell AC, Felsenfeld G. Methylation of a CTCF-dependent boundary controls imprinted expression of the Igf2 gene. Nature. 2000; 405:482–485. [PubMed: 10839546]

2. Dallas NA, Xia L, Fan F, Gray MJ, Gaur P, van Buren G 2, et al. Chemoresistant colorectal cancer cells, the cancer stem cell phenotype, and increased sensitivity to insulin-like growth factor-I receptor inhibition. Cancer research. 2009; 69:1951–1957. [PubMed: 19244128]

3. Desbois-Mouthon C, Cacheux W, Blivet-Van Eggelpoel MJ, Barbu V, Fartoux L, Poupon R, et al. Impact of IGF-1R/EGFR cross-talks on hepatoma cell sensitivity to gefitinib. Int J Cancer. 2006; 119:2557–2566. [PubMed: 16988945]

4. Dhe-Paganon S, Syeda F, Park L. DNA methyl transferase 1: regulatory mechanisms and implications in health and disease. Int J Biochem Mol Biol. 2011; 2:58–66. [PubMed: 21969122]

5. Duvic M, Talpur R, Ni X, Zhang C, Hazarika P, Kelly C, et al. Phase 2 trial of oral vorinostat (suberoylanilide hydroxamic acid, SAHA) for refractory cutaneous T-cell lymphoma (CTCL). Blood. 2007; 109:31–39. [PubMed: 16960145]

6. Eckstein N, Servan K, Hildebrandt B, Politz A, von Jonquieres G, Wolf-Kummeth S, et al. Hyperactivation of the insulin-like growth factor receptor I signaling pathway is an essential event for cisplatin resistance of ovarian cancer cells. Cancer research. 2009; 69:2996–3003. [PubMed: 19318572]

7. Fantin VR, Richon VM. Mechanisms of resistance to histone deacetylase inhibitors and their therapeutic implications. Clin Cancer Res. 2007; 13:7237–7242. [PubMed: 18094401]

8. Fantin VR, Loboda A, Paweletz CP, Hendrickson RC, Pierce JW, Roth JA, et al. Constitutive activation of signal transducers and activators of transcription predicts vorinostat resistance in cutaneous T-cell lymphoma. Cancer research. 2008; 68:3785–3794. [PubMed: 18483262]

9. Garcia-Manero G, Yang H, Bueso-Ramos C, Ferrajoli A, Cortes J, Wierda WG, et al. Phase 1 study of the histone deacetylase inhibitor vorinostat (suberoylanilide hydroxamic acid [SAHA]) in patients with advanced leukemias and myelodysplastic syndromes. Blood. 2008; 111:1060–1066. [PubMed: 17962510]

10. Hark AT, Schoenherr CJ, Katz DJ, Ingram RS, Levorse JM, Tilghman SM. CTCF mediates methylation-sensitive enhancer-blocking activity at the H19/Igf2 locus. Nature. 2000; 405:486–489. [PubMed: 10839547]

11. Huang GS, Brouwer-Visser J, Ramirez MJ, Kim CH, Hebert TM, Lin J, et al. Insulin-like growth factor 2 expression modulates Taxol resistance and is a candidate biomarker for reduced disease-free survival in ovarian cancer. Clin Cancer Res. 2010; 16:2999–3010. [PubMed: 20404007]

12. Jin Q, Lee HJ, Min HY, Smith JK, Hwang SJ, Whang YM, et al. Transcriptional and posttranslational regulation of insulin-like growth factor binding protein-3 by Akt3. Carcinogenesis. 2014

13. Kim JS, Lee SC, Min HY, Park KH, Hyun SY, Kwon SJ, et al. Activation of insulin-like growth factor receptor signaling mediates resistance to histone deacetylase inhibitors. Cancer Lett. 2015

14. Kirschbaum M, Gojo I, Goldberg SL, Bredeson C, Kujawski LA, Yang A, et al. A phase 1 clinical trial of vorinostat in combination with decitabine in patients with acute myeloid leukaemia or myelodysplastic syndrome. British journal of haematology. 2014; 167:185–193. [PubMed: 25040094]

15. Kohda M, Hoshiya H, Katoh M, Tanaka I, Masuda R, Takemura T, et al. Frequent loss of imprinting of IGF2 and MEST in lung adenocarcinoma. Mol Carcinog. 2001; 31:184–191. [PubMed: 11536368]

16. Lawson EA, Zhang X, Crocker JT, Wang WL, Klibanski A. Hypoglycemia from IGF2 overexpression associated with activation of fetal promoters and loss of imprinting in a metastatic hemangiopericytoma. The Journal of clinical endocrinology and metabolism. 2009; 94:2226–2231. [PubMed: 19383775]

17. Lee H, Zhang P, Herrmann A, Yang C, Xin H, Wang Z, et al. Acetylated STAT3 is crucial for methylation of tumor-suppressor gene promoters and inhibition by resveratrol results in demethylation. Proceedings of the National Academy of Sciences of the United States of America. 2012; 109:7765–7769. [PubMed: 22547799]

18. Lee JH, Choy ML, Marks PA. Mechanisms of resistance to histone deacetylase inhibitors. Advances in cancer research. 2012; 116:39–86. [PubMed: 23088868]

19. Lee JS, Kang JH, Boo HJ, Hwang SJ, Hong S, Lee SC, et al. STAT3-mediated IGF-2 secretion in the tumour microenvironment elicits innate resistance to anti-IGF-1R antibody. Nat Commun. 2015; 6:8499. [PubMed: 26465273]

20. Licciardi PV, Ververis K, Tang ML, El-Osta A, Karagiannis TC. Immunomodulatory effects of histone deacetylase inhibitors. Curr Mol Med. 2013; 13:640–647. [PubMed: 23061676]

21. Livak KJ, Schmittgen TD. Analysis of relative gene expression data using real-time quantitative PCR and the 2(T)(-Delta Delta C) method. Methods. 2001; 25:402–408. [PubMed: 11846609]

22. Lui JC, Baron J. Evidence that Igf2 down-regulation in postnatal tissues and up-regulation in malignancies is driven by transcription factor E2f3. Proceedings of the National Academy of Sciences of the United States of America. 2013; 110:6181–6186. [PubMed: 23530192]

23. Mathelier A, Zhao X, Zhang AW, Parcy F, Worsley-Hunt R, Arenillas DJ, et al. JASPAR 2014: an extensively expanded and updated open-access database of transcription factor binding profiles. Nucleic acids research. 2014; 42:D142–147. [PubMed: 24194598]

24. Mayo MW, Denlinger CE, Broad RM, Yeung F, Reilly ET, Shi Y, et al. Ineffectiveness of histone deacetylase inhibitors to induce apoptosis involves the transcriptional activation of NF-kappa B through the Akt pathway. J Biol Chem. 2003; 278:18980–18989. [PubMed: 12649266]

25. McCue J, Freed B. Measuring lymphocyte transcription factor activity by ELISA. Current protocols in toxicology / editorial board, Mahin D Maines. 2005; Chapter 18(Unit18):15.

26. Min HY, Yun HJ, Lee JS, Lee HJ, Cho J, Jang HJ, et al. Targeting the insulin-like growth factor receptor and Src signaling network for the treatment of non-small cell lung cancer. Mol Cancer. 2015; 14:113. [PubMed: 26041671]

27. Minucci S, Pelicci PG. Histone deacetylase inhibitors and the promise of epigenetic (and more) treatments for cancer. Nature Reviews Cancer. 2006; 6:38–51. [PubMed: 16397526]

28. Nordin M, Bergman D, Halje M, Engstrom W, Ward A. Epigenetic regulation of the Igf2/H19 gene cluster. Cell proliferation. 2014; 47:189–199. [PubMed: 24738971]

29. O'Connor OA, Heaney ML, Schwartz L, Richardson S, Willim R, MacGregor-Cortelli B, et al. Clinical experience with intravenous and oral formulations of the novel histone deacetylase inhibitor suberoylanilide hydroxamic acid in patients with advanced hematologic malignancies. J Clin Oncol. 2006; 24:166–173. [PubMed: 16330674]

30. Olsen EA, Kim YH, Kuzel TM, Pacheco TR, Foss FM, Parker S, et al. Phase IIb multicenter trial of vorinostat in patients with persistent, progressive, or treatment refractory cutaneous T-cell lymphoma. J Clin Oncol. 2007; 25:3109–3115. [PubMed: 17577020]

31. Phillips JE, Corces VG. CTCF: master weaver of the genome. Cell. 2009; 137:1194–1211. [PubMed: 19563753]

32. Sakatani T, Kaneda A, Iacobuzio-Donahue CA, Carter MG, de Boom Witzel S, Okano H, et al. Loss of imprinting of Igf2 alters intestinal maturation and tumorigenesis in mice. Science. 2005; 307:1976–1978. [PubMed: 15731405]

33. Schneider CA, Rasband WS, Eliceiri KW. NIH Image to ImageJ: 25 years of image analysis. Nature methods. 2012; 9:671–675. [PubMed: 22930834]

34. Schoenherr CJ, Levorse JM, Tilghman SM. CTCF maintains differential methylation at the Igf2/H19 locus. Nat Genet. 2003; 33:66–69. [PubMed: 12461525]

35. Schust J, Sperl B, Hollis A, Mayer TU, Berg T. Stattic: a small-molecule inhibitor of STAT3 activation and dimerization. Chemistry & biology. 2006; 13:1235–1242. [PubMed: 17114005]

36. Shan J, Shen J, Liu L, Xia F, Xu C, Duan G, et al. Nanog regulates self-renewal of cancer stem cells through the insulin-like growth factor pathway in human hepatocellular carcinoma. Hepatology. 2012; 56:1004–1014. [PubMed: 22473773]

37. Shin DH, Min HY, El-Naggar AK, Lippman SM, Glisson B, Lee HY. Akt/mTOR counteract the antitumor activities of cixutumumab, an anti-insulin-like growth factor I receptor monoclonal antibody. Mol Cancer Ther. 2011; 10:2437–2448. [PubMed: 21980128]

38. Shin DH, Lee HJ, Min HY, Choi SP, Lee MS, Lee JW, et al. Combating resistance to anti-IGFR antibody by targeting the integrin beta3-Src pathway. J Natl Cancer Inst. 2013; 105:1558–1570. [PubMed: 24092920]

39. Singh P, Dai B, Given RL, Lu X, Holthuizen PE. Differential activation of IGF-II promoters P3 and P4 in Caco-2 cells during growth and differentiation. Gastroenterology. 1998; 114:1221–1229. [PubMed: 9609759]

40. Suzuki H, Ueda R, Takahashi T. Altered imprinting in lung cancer. Nat Genet. 1994; 6:332–333. [PubMed: 8054970]

41. Tada Y, Yamaguchi Y, Kinjo T, Song X, Akagi T, Takamura H, et al. The stem cell transcription factor ZFP57 induces IGF2 expression to promote anchorage-independent growth in cancer cells. Oncogene. 2015; 34:752–760. [PubMed: 24469060]

42. Traynor AM, Dubey S, Eickhoff JC, Kolesar JM, Schell K, Huie MS, et al. Vorinostat (NSC# 701852 in patients with relapsed non-small cell lung cancer: a Wisconsin Oncology Network phase II study. J Thorac Oncol. 2009; 4:522–526. [PubMed: 19347984]

43. van Dijk MA, van Schaik FM, Bootsma HJ, Holthuizen P, Sussenbach JS. Initial characterization of the four promoters of the human insulin-like growth factor II gene. Molecular and cellular endocrinology. 1991; 81:81–94. [PubMed: 1797589]

44. Villanueva J, Vultur A, Lee JT, Somasundaram R, Fukunaga-Kalabis M, Cipolla AK, et al. Acquired resistance to BRAF inhibitors mediated by a RAF kinase switch in melanoma can be overcome by cotargeting MEK and IGF-1R/PI3K. Cancer Cell. 2010; 18:683–695. [PubMed: 21156289]

45. Wang K, Wang C, Xiao F, Wang H, Wu Z. JAK2/STAT2/STAT3 are required for myogenic differentiation. J Biol Chem. 2008; 283:34029–34036. [PubMed: 18835816]

46. Wang X, Crowe PJ, Goldstein D, Yang JL. STAT3 inhibition, a novel approach to enhancing targeted therapy in human cancers (review). International journal of oncology. 2012; 41:1181–1191. [PubMed: 22842992]

47. Yee D. Insulin-like growth factor receptor inhibitors: baby or the bathwater? J Natl Cancer Inst. 2012; 104:975–981. [PubMed: 22761272]

48. Yu H, Lee H, Herrmann A, Buettner R, Jove R. Revisiting STAT3 signalling in cancer: new and unexpected biological functions. Nat Rev Cancer. 2014; 14:736–746. [PubMed: 25342631]

49. Yuan ZL, Guan YJ, Chatterjee D, Chin YE. Stat3 dimerization regulated by reversible acetylation of a single lysine residue. Science. 2005; 307:269–273. [PubMed: 15653507]

50. Zhang X, Guo C, Chen Y, Shulha HP, Schnetz MP, LaFramboise T, et al. Epitope tagging of endogenous proteins for genome-wide ChIP-chip studies. Nature methods. 2008; 5:163–165. [PubMed: 18176569]
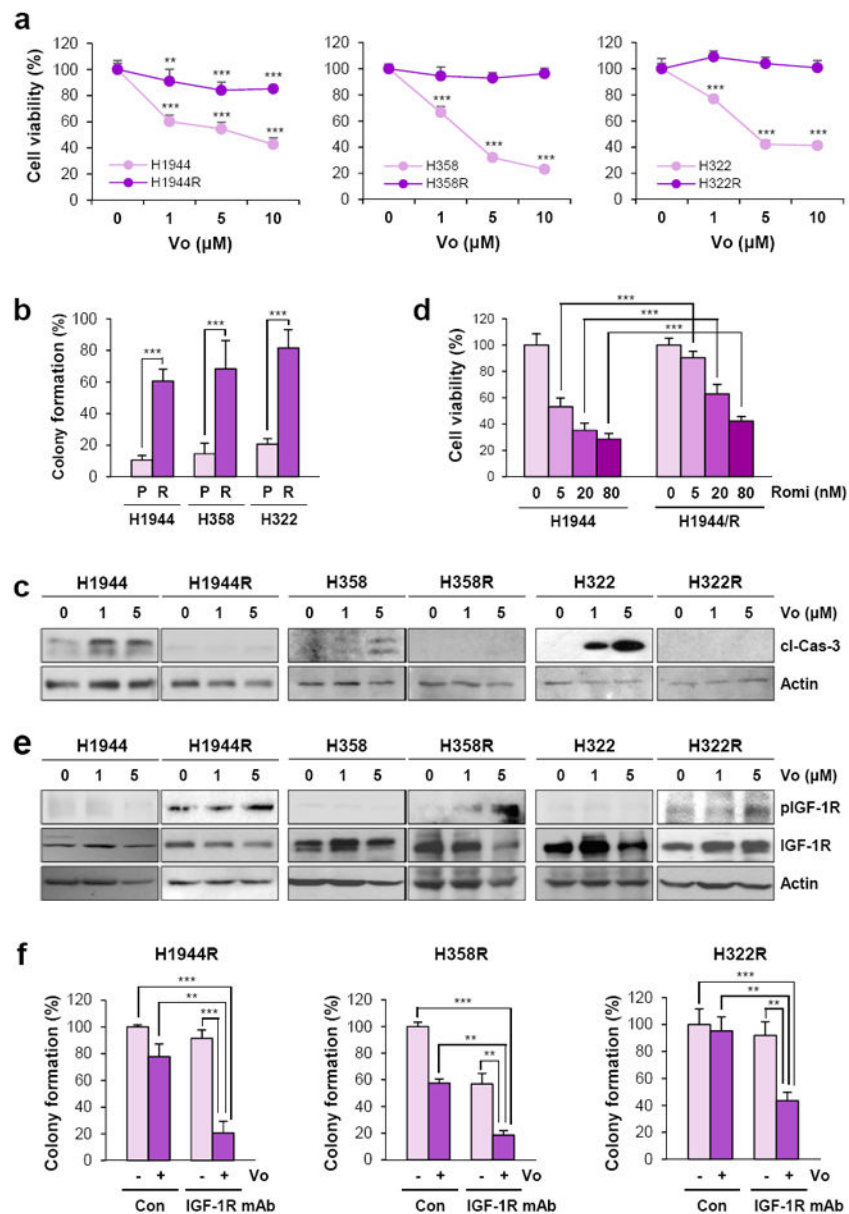
Figure 1. The involvement of the IGF-1R pathway in acquired vorinostat resistance

(a and b) The effects of vorinostat on the viability (a) and anchorage-independent colony formation (b) of the indicated NSCLC cell lines and their corresponding acquired VoR sublines. (a) Cell viability was determined by the MTT assay ($n = 3$). (b) The soft agar colony formation assay was performed to evaluate the effect of 1 μM vorinostat on anchorage-independent colony formation. Data indicates the percentage of colony formation in vorinostat-treated cells compared with vehicle-treated control cells ($n = 3$). (c) Immunoblots comparing the expression of cleaved caspase-3 (cl-Cas-3) between the indicated parental and VoR sublines. Cells were treated with vorinostat for 2 days. (d) The MTT assay evaluating the effect of romidepsin (Romi) on the viability of H1944 and H1944R cells. Cells were treated with indicated concentrations of romidepsin for 3 days ($n =$

3). (e) The expression levels of total and phosphorylated IGF-1R in the indicated NSCLC cells were determined by Western blot analysis. Cells were treated with vorinostat for 2 days. (f) Anchorage-independent colony formation assay evaluating vorinostat resistance of the indicated cells with combined treatment with vorinostat (1 μM) and an IGF-1R mAb (1 μg/ml) ($n = 3$). **: $P < 0.01$; ***: $P < 0.001$, analyzed by two-sided Student's t-test. Vo: vorinostat; Con: control.
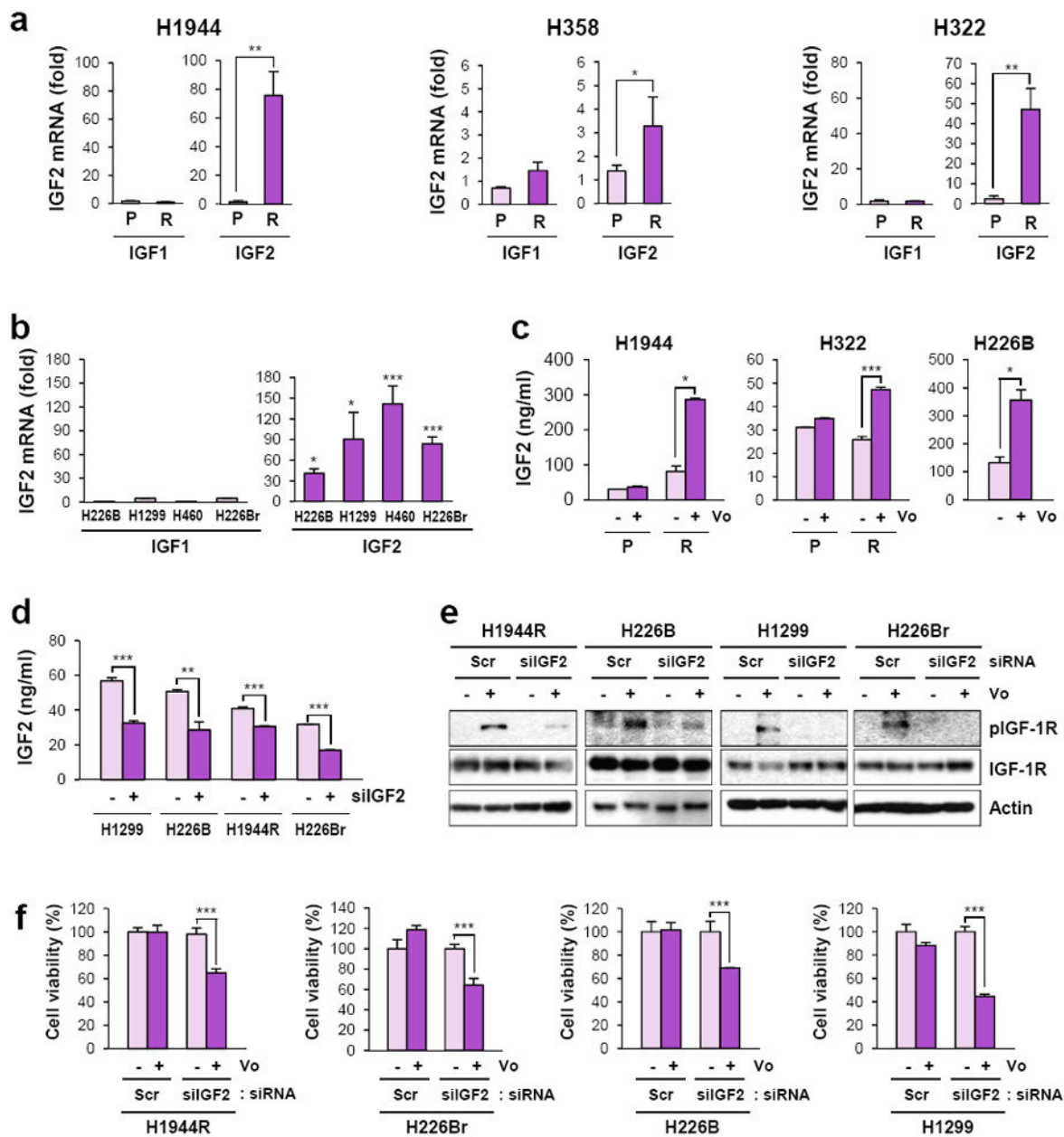
Figure 2. Activation of IGF-1R caused by increased *IGF2* transcription in NSCLC cells with vorinostat resistance

(a and b) Real-time PCR assays analyzing the relative amounts of *IGF1* and *IGF2* transcription in the indicated parental (P) and their corresponding VoR sublines (a) and in various NSCLC cell lines with primary vorinostat resistance (b) by treatment with vorinostat (5 μM) for 2 days. Data indicates the fold increases of mRNA levels in vorinostat-treated cells compared with vehicle-treated control cells (*n* = 3). (c) Determination of vorinostat-induced IGF2 production by ELISA (*n* = 3). The conditioned mediums (CMs) obtained from cells treated with vorinostat (5 μM) for 2 days were used for ELISA. (d) Decreases in IGF2 levels in the CMs after silencing IGF2 expression using siRNAs, determined by ELISA (*n* = 3). Cells were transfected with scrambled or IGF2 siRNAs for 6 h. The CMs were collected

48 h after transfection. (e) Immunoblots of total and phosphorylated IGF-1R expression in the indicated NSCLC cells with siRNA-mediated silencing of IGF2 expression and vorinostat (5 μM) treatment for 2 days. Cells were transfected with IGF2 siRNAs, and then treated with vorinostat. (e) The MTT assay evaluating the effects of vorinostat on the viability of indicated NSCLC cell lines with siRNA-mediated silencing of IGF2 expression ($n = 3$). IGF2 siRNA-transfected cells were reseeded into 96 well plates and then treated with vorinostat (5 μM) for 3 days. *: $P < 0.05$; **: $P < 0.01$; ***: $P < 0.001$, analyzed by two-sided Student's t-test. Vo: vorinostat.
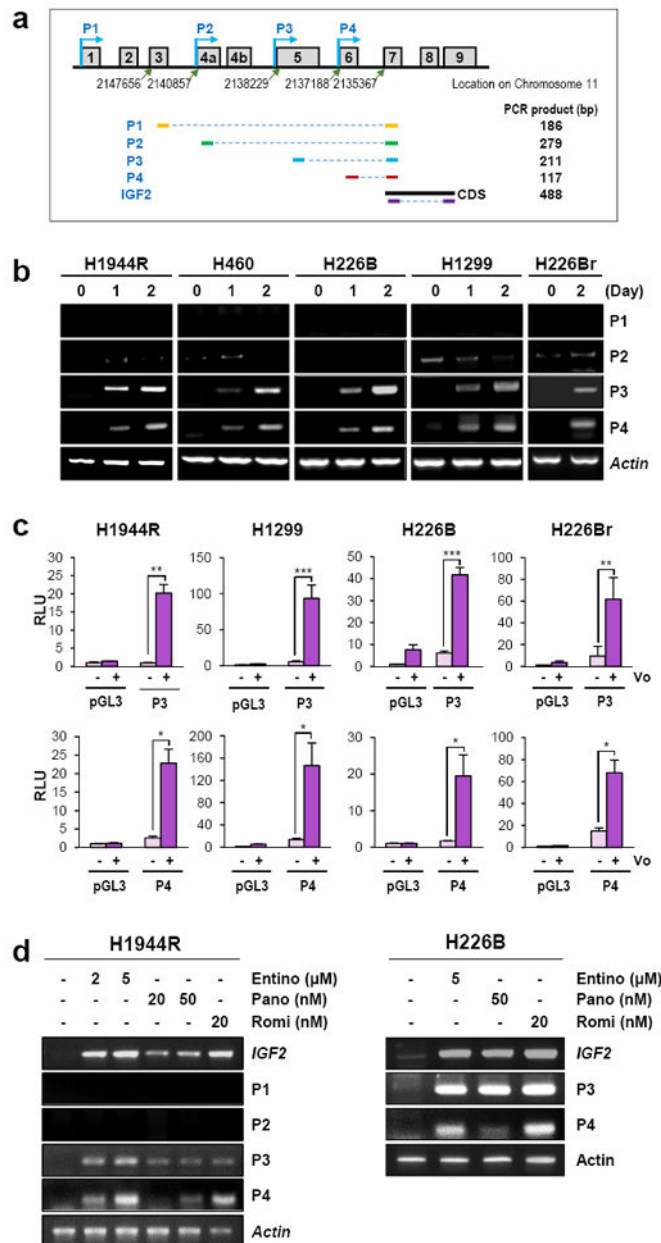
Figure 3. Vorinostat-mediated increase in *IGF2* transcription by activation of *IGF2* P3 and/or P4 promoter in vorinostat-resistant NSCLC cells

(a) Schematic diagram of *IGF2* promoters. Four alternate promoter sites are labeled P1–P4. Locations of exons 3, 4a, 5, 6, and 7 were determined by comparison with the GenBank sequence database (Chromosome 11; the reference genome assembly: GRCh38.p2) using BLAST. The PCR primers for promoter-specific transcripts of *IGF2*, the *IGF2* transcript amplifying the coding sequence (CDS) region, and the predicted size of PCR products for transcripts produced using each five set of primers are presented below the schematic diagram. (b) RT-PCR analysis on actual PCR products for *IGF2* transcripts from each of the four promoters in the indicated cell lines treated with vorinostat (5 μM) for 2 days. (c) Luciferase reporter assay evaluating the vorinostat-mediated *IGF2* P3 (upper) and P4 (lower)

promoter activities in cells treated with vorinostat (5 μM) for 2 days ($n = 3$). (d) RT PCR assay analyzing IGF2 mRNA expression in H1944R and H226B cells by treatment with entinostat (Entino), panobinostat (Pano), and romidepsin (Romi) for 2 days. *: $P < 0.05$; **: $P < 0.01$; ***: $P < 0.001$, analyzed by two-sided Student's t-test. Vo: vorinostat. RLU: relative luminescence units.
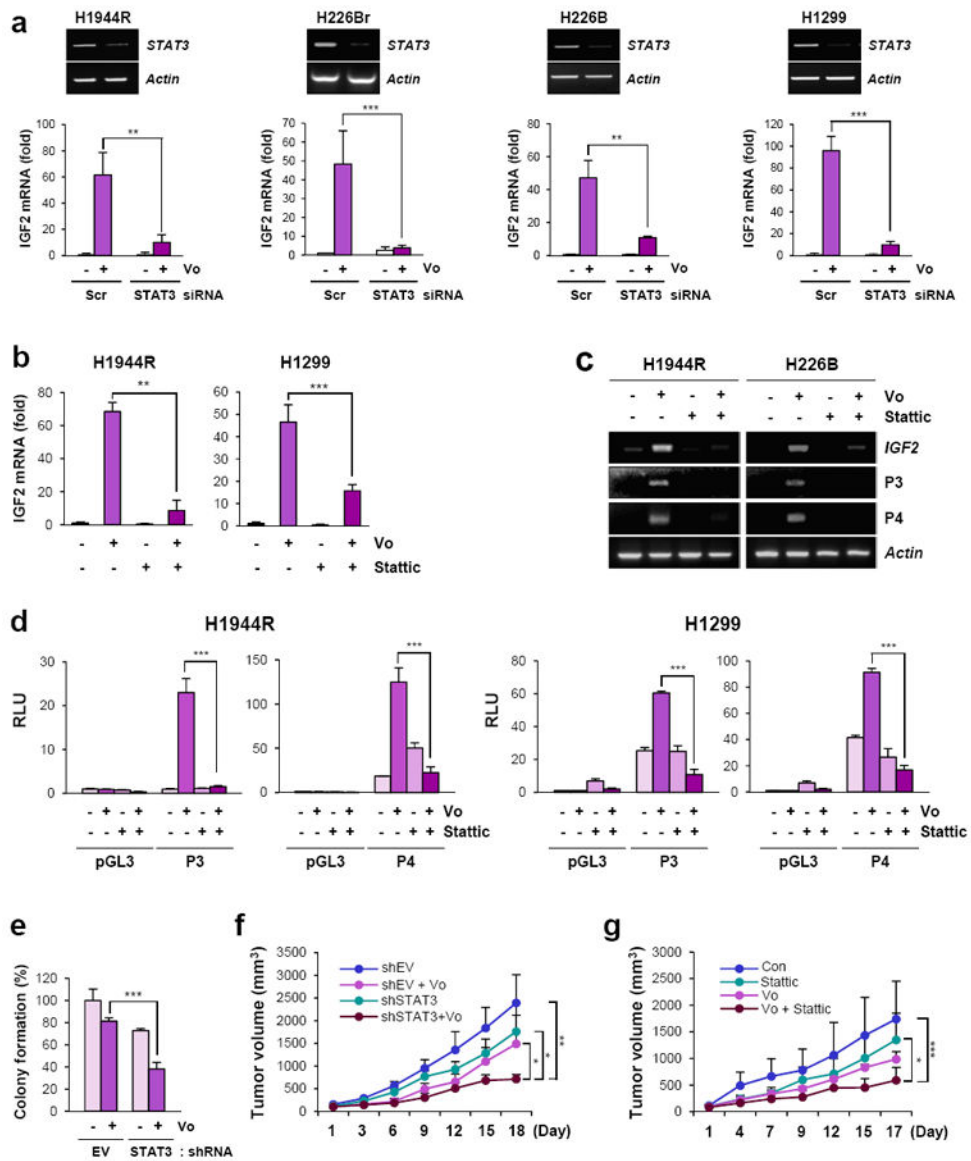
Figure 4. Association of STAT3 with vorinostat resistance via activating P3 and P4 promoters-driven *IGF2* transcription

(a) Real-time PCR analyzing the siRNA-mediated silencing of STAT3 expression on vorinostat-induced *IGF2* transcription in the indicated NSCLC cell lines. Cells were treated with vorinostat (5 μM) for 2 days (*n* = 3). *Up.* The silencing of STAT3 transcription after transfection with STAT3-specific siRNAs was determined by RT-PCR. (b) Real-time PCR analyzing IGF2 mRNA expression in the indicated cells after treatment with Stattic (5 μM), vorinostat (5 μM), or their combination for 2 days (*n* = 3). (c) RT–PCR for analyzing IGF2 mRNA expression and the promoter-specific *IGF2* transcription in the indicated cells after treatment with Stattic, vorinostat, or their combination for 2 days. (d) Luciferase reporter assay analysing attenuation of vorinostat-mediated increases in the promoter activity of *IGF2* P3 and P4 promoters by combined treatment with Stattic (5 μM) for 2 days (*n* = 3). (e) Enhanced inhibitory effect of vorinostat (1 μM) on the anchorage-dependent colony

formation of H1299 cells expressing stably depleted STAT3 levels ($n = 3$). (f and g) Enhanced antitumor effects of vorinostat (50 mg/kg) on xenograft tumors of H1299 cells expressing stably depleted STAT3 levels ($n = 4$) (f) or on the NSCLC patient-derived xenografts (PDXs) by combinatorial treatment with Stattic (50 mg/kg) ($n = 7$) (g). *: $P < 0.05$; **: $P < 0.01$; ***: $P < 0.001$, analyzed by two-sided Student's t-test (a, b, d, e) or one-way ANOVA (f). Vo: vorinostat. RLU: relative luminescence units.
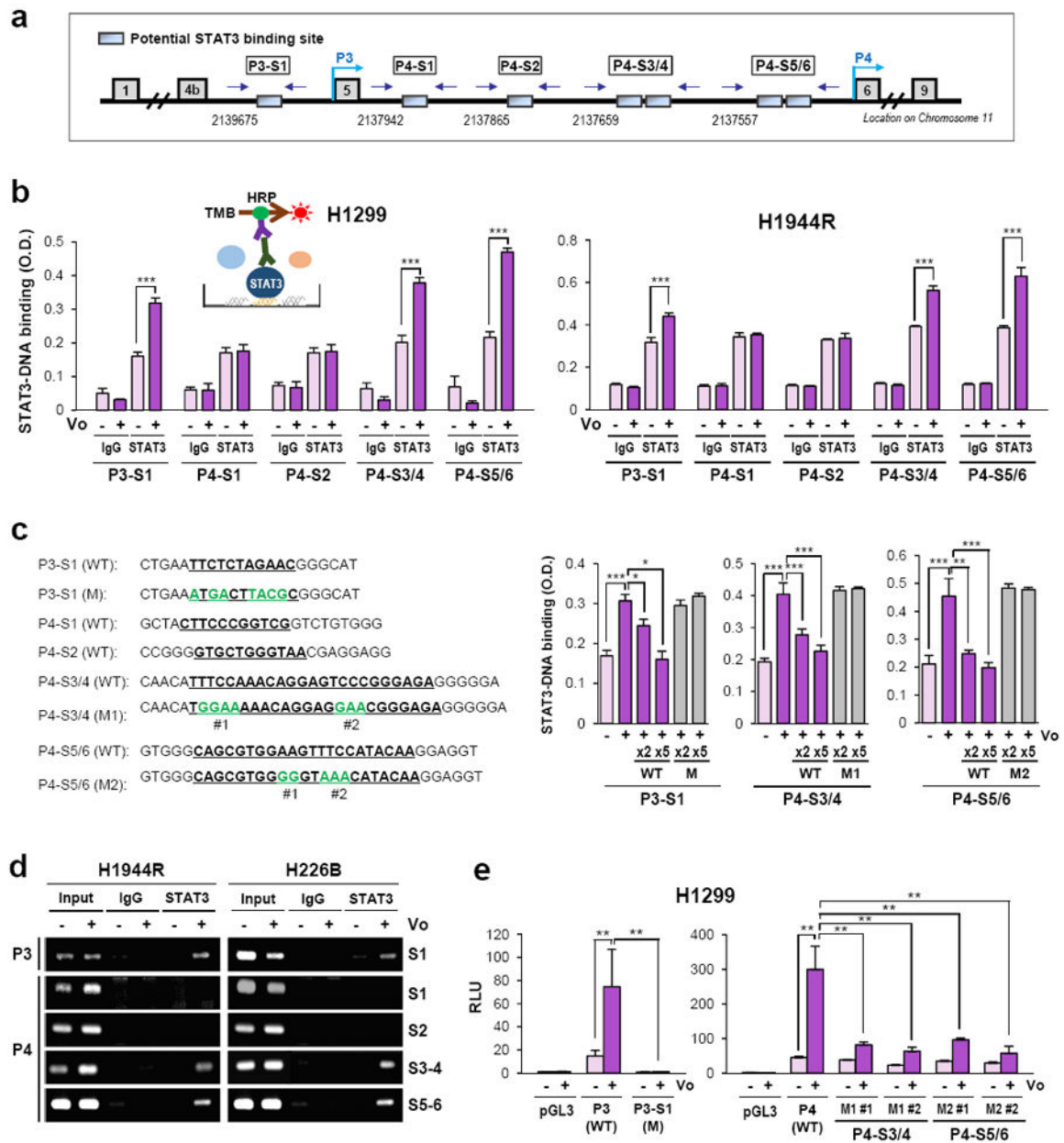
Figure 5. Direct binding of STAT3 to *IGF2* P3 and P4 promoters

(a and c) Schematic of the seven potential STAT-binding sites in *IGF2* P3 and P4 promoters (P3-S1 located in promoter 3 and P4-S1 to P4-S6 located in promoter 4) predicted by the JASPAR database. (c) The wild-type (WT) and mutant (M) DNA sequences for the putative STAT3-binding sites in *IGF2* P3 and P4 promoters. #1 and #2 indicate the mutation of each potential STAT3 binding site of P4-S3/4 and P4-S5/6 in (e). Locations were determined by comparison with the GenBank sequence database (Chromosome 11; the reference genome assembly: GRCh38.p2) using BLAST. (b-d) Direct STAT3 binding to the putative STAT3-binding sites after treatment with vorinostat (5 μM) for 2 days, evaluated by the DNA ELISA assay (b) using the oligomers carrying the DNA sequences indicated in (c) (*n* = 3)

and by ChIP assay (d) using the PCR primers encompassing the putative STAT3-binding sites indicated in (a) by arrows. Specificity of the binding in the ELISA assay was determined by pre-incubating the cell lysates with 2- and 5-fold excess amounts of WT or mutant (M) STAT3 oligomers (c, right). (e) Luciferase reporter assay evaluating the effects of vorinostat (5 μM) on *IGF2* promoters 3 and 4 carrying WT or mutations in the putative STAT3-binding sites described in (c) ($n = 3$). Cells were treated with vorinostat for 2 days. *: $P < 0.05$; **: $P < 0.01$; ***: $P < 0.001$, analyzed by two-sided Student's *t*-test. Vo: vorinostat.
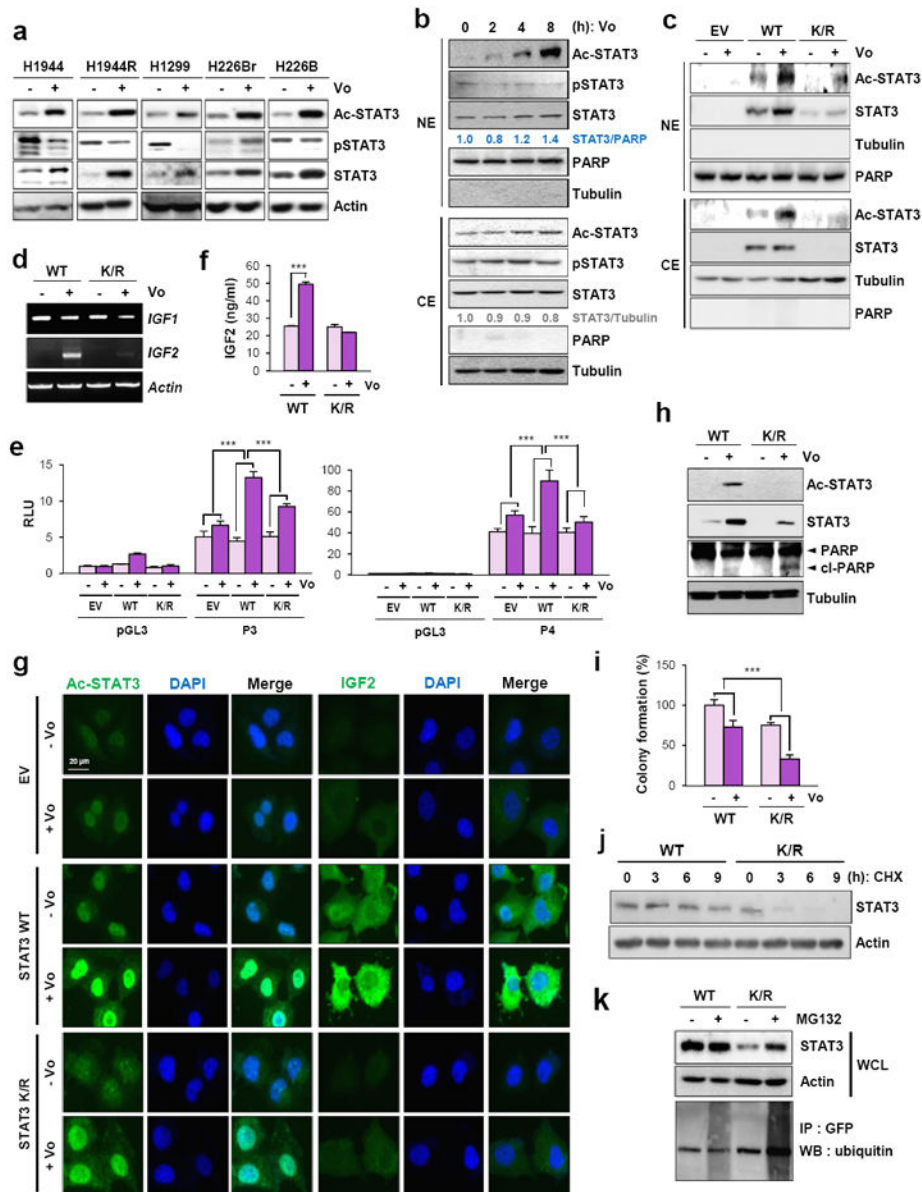
Figure 6. Acetylated STAT3 by vorinostat treatment leads to stabilization, thereby mediating vorinostat-induced *IGF2* transcription

(a) Immunoblots evaluating the expression of acetylated, phosphorylated, and total STAT3 in indicated cells treated with vorinostat (5 μM) for 2 days. (b) Immunoblots evaluating the expression of acetylated (Ac-STAT3), phosphorylated (pSTAT3), and total STAT3 in the cytosol or nuclear compartments of H1299 cells upon vorinostat treatment for the indicated time periods. The numbers below STAT3 blots indicate densitometry of STAT3 blots normalized by loading controls (nuclear compartment: PARP, cytosolic compartment: tubulin). Densitometric analysis was performed using Image J software. (c) Immunoblots evaluating nuclear (NE) and cytosolic (CE) expression of STAT3 and Ac-STAT3 after the vorinostat treatment (5 μM) in H1299 cells expressing WT or mutant (K/R) STAT3 for 36 h. (d-g) The role of STAT3 acetylation in vorinostat-mediated IGF2 expression in H1299 cells

expressing WT or mutant (K/R) STAT3. Cells were treated with vorinostat (5 μM) for 2 days. (d) RT–PCR analysis evaluating the vorinostat-mediated IGF2 mRNA expression in H1299 cells expressing WT or mutant (K/R) STAT3. (e) Activation of *IGF2* P3 (left) and P4 (right) promoters was analyzed by luciferase reporter assay after vorinostat treatment (n = 3). (f) The IGF2 secretion in CMs obtained from vorinostat-treated cells was determined by ELISA (n = 3). (g) Immunofluorescence staining of Ac-STAT3 and IGF2 after vorinostat treatment. (h) Western blot analysis evaluating total and acetylated STAT3 expressions and PARP cleavage in H1299 cells expressing WT or mutant (K/R) STAT3 after treatment with vorinostat (5 μM) for 2 days. (i) Enhanced inhibitory effects of vorinostat (1 μM) on the anchorage-dependent colony formation of H1299 cells expressing stably depleted STAT3 levels (n = 3). (j) Immunoblots evaluating the half-life of wild type (WT) and mutant (K/R) STAT3 protein after treatment with cycloheximide (100 μg/ml) for the indicated time points. (k) The level of wild type (WT) and mutant (K/R) STAT3 ubiquitination in H1299 cells was determined by immunoprecipitation (IP) with a GFP antibody and western blot analysis (WB) with an antibody against ubiquitin. Immunoblots determining the STAT3 expression in whole cell lysates (WCL) are included. ***: $P < 0.001$, analyzed by two-sided Student's t-test. Vo: vorinostat. RLU: relative luminescence units. Ub: ubiquitin.